BJES Basrah Journal for Engineering Sciences

Basrah Journal for Engineering Sciences, Vol. 22, No. 2, (2022), 80-89

Original Article

Journal homepage: www.bjes.edu.iq
ISSN (Online): 23118385, ISSN (Print): 18146120

OPEN ACCESS

Behaviour of New Curved in Plan Composite Reinforced Concrete Beams

Dolfocar Ali Usamah Witwit [1,*], Nabeel Abdulrazzaq Jasim [2]

[1,2] *Department of Civil Engineering, College of Engineering, University of Basrah, Basrah, Iraq*
E-mail addresses: my_maile90@yahoo.com , nabeel_ali58@yahoo.com
Received: 12 May 2022; Accepted: 13 June 2022; Published: 24 December 2022

Abstract

New composite reinforced concrete beams, in which reinforced concrete component is connected to steel T-section, are proposed. The stirrups of the beam were utilized as shear connectors by passing them through drilled holes in the web of the steel T-section. Experimental test and numerical analysis were conducted to determine the behaviour of such beams when subjected to combined shear, torsion, and bending stresses. Full scale one conventional reinforced concrete curved in plan beam C1, and four composite reinforced concrete ones, C2 to C5, were tested. The degree of shear connection between the two components of beams C2 to C5 was changed by varying the number of stirrups which are used as shear connectors. The increase in load carrying capacity of the composite reinforced concrete beams reached 55 % for beam C4 as compared to that of ordinary reinforced concrete beam. The experimental results demonstrated that the stirrups are very effective in providing the interaction between the two components of the beams. The degree of shear connection emerged not to have effect on the behaviour of tested beams. Three-dimensional finite element analysis was conducted using commercial software ABAQUS. To model the shear connection in composite reinforced concrete beam, the stirrups were connected to the web of the steel T-section by springs at the location of the stirrups. Good agreement is obtained between the results of the experimental tests and the finite element analysis.

Keywords: Composite reinforced concrete beams, Composite sections, Curved beams, Shear connection.

https://doi.org/10.33971/bjes.22.2.12

1. Introduction

The method of combining steel and reinforced concrete, designated composite reinforced concrete CRC, was proposed in 1971 [1]. It was so called since it is a combination of composite construction and reinforced concrete.

In any comparison of different construction modes, the total cost, including the cost of the structural material and the cost of construction, is the governing matter. CRC combines the material advantages of reinforced concrete with the constructional advantages of normal composite construction [2]. From material viewpoint the reinforced concrete is cheaper because the steel, the most expensive material, is used much more efficiently close to the soffit of beam. However, from the construction viewpoint, normal composite construction is the cheaper because the steel framework can be quickly built and used in constructing the concrete floor, especially when precast units or profiled steel sheets are used to spanning between the steel beams to act as formwork [1].

The cross section of a CRC beam consists of a steel channel at the soffit of the beam connected to reinforced concrete by shear connectors, Fig. 1 (a). The shear connectors may be conventional studs welded to the web of channel section, transvers bolts [1] passing through holes in the flanges of the channel or transvers bars [2] placed through holes in the flanges of the channel.

Although the number of shear connectors was reduced in CRC compared to normal composite construction, however, their cost is quite large. Recently, new form of CRC has been proposed [3]. In the new structural material, the steel channel section was replaced by steel T-section and the shear stirrups of reinforced concrete were utilized to act as shear connectors. The steel T-section is better than the channel section in supporting the form for casting the concrete floor. Also, while in the new system no additional shear connectors are required, the preparation for connecting the steel T-section to the reinforced concrete needs only drilled holes in the web of the steel T-section through which the stirrups pass. To facilitate the construction, each stirrup was made from two C-shaped parts as shown in Fig. 1 (b).

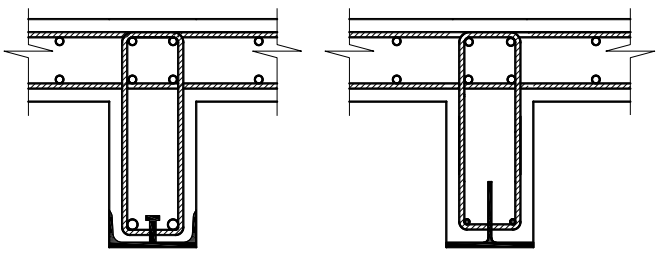

(a) Taylor's section (b) Proposed section

Fig. 1 CRC section.

Witwit and Jasim [4] investigated the behaviour under sagging and hogging bending moments of beams made of the proposed new CRC. The beams were tested under four-point

loading. The effect on bending strength of beams of different degrees of shear connection was investigated. Also, the behaviour of the proposed section under pure torsion was investigated for two degrees of shear connection by Witwit and Jasim [5].

Curved in plan beams have already been encountered in buildings and highway bridges. These members are subjected to combined flexure and torsion. There are no experimental studies on behaviour of CRC beams under combined flexure and torsion. However, experimental tests as well as numerical analyses were conducted on normal composite steel-concrete beams subjected to combined flexure and torsion [6]-[10]. Straight and curved beams were investigated under such combined loading and for both full and partial shear connections. The results illustrated that the presence of flexure leads to an increase in the torsional moment capacity, but the flexural moment capacity dose not increase in the presence of torsion. Also, it was found that beams with partial shear connection achieve a similar strength compared to those with full shear connection.

In normal composite beams under torsion, the contribution of the steel I-section towards the torsional strength of the composite beam was neglected [11] Hence, the torsional strength of such beams was determined as strength of the concrete slab only.

This paper describes tests conducted on curve in plan beams made of the new CRC under concentrated load at mid span. The behaviour and strength of such beams are attempted to be determined experimentally. Nonlinear finite element analysis is also conducted to study the behaviour of the beams up to failure. The results of the finite element analysis are compared with those obtained from the experimental tests.

2. Experimental work

2.1. Test beams

As a part of this study, experimental tests were conducted on four full scale CRC beams and one ordinary reinforced concrete RC beam curved in plan to investigate the behaviour of the beams. Each beam has a length of 3 m with effective span of 2.6 m. The cross section of the beams was rectangular of 175 mm width and 350 mm depth. The cross section of CRC beams was designed to be able to resist a positive (sagging) bending moment of 73.5 kN.m, a negative (hogging) bending moment of 93.87 kN.m, a shearing force of 125 kN and twisting moment of 12.70 kN.m. These values of the applied moments and forces were determined by applying a load of 250 kN at mid-span of horizontally circular curved beam with 1650 mm radius [3]. The beam was analyzed elastically as illustrated in Appendix 1. The cross section of beams was designed as singly reinforced concrete according to the requirements of ACI318-14 code [17]. The steel T-section was considered as a traditional reinforcement. The effective depth of the section for the positive bending moment was calculated to the centroid of the T-section. The details of tested beams are shown in Table 1 and Figs. 2 and 3.

The stirrups were designed for combined shear and torsion and were made in two types, the first is a two-piece C-shaped stirrup that pass through the web of the steel T-section, the other type is a one part closed stirrup that do not pass through the web of the steel T-section, Fig. 2. When all stirrups were used as shear connectors, as in beam C2, it was designated as beam with 100 % degree of shear connection. The total number of stirrups was 43. To change the degree of shear connection, alternate stirrups were used as connectors in beams C4 resulting in a total of 21 stirrup connectors and 22 closed stirrups that do not pass through the web. This beam was designated as beam with 48.8 % (= 21/43 × 100) degree of shear connection. Similarly, the degree of shear connection for beams C3 and C5 were calculated where the number of stirrup connectors were 29 and 11 respectively. The stirrup distribution through the length of the beam is shown in Fig. 2.

Table 1. Description of the specimens.

Specimen designation	Degree of shear connection (No. of stirrup connectors)	Dimensions (mm)		
		Depth	Width	Radius
C1	R.C	350	175	1650
C2	100 (43)	350	175	1650
C3	67 (29)	350	175	1650
C4	49 (21)	350	175	1650
C5	26 (11)	350	175	1650

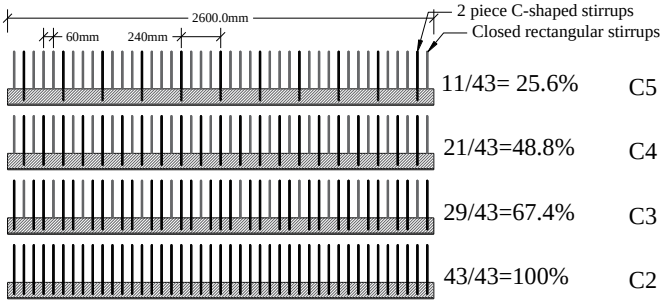

Fig. 2 Stirrup distribution for the tested beams.

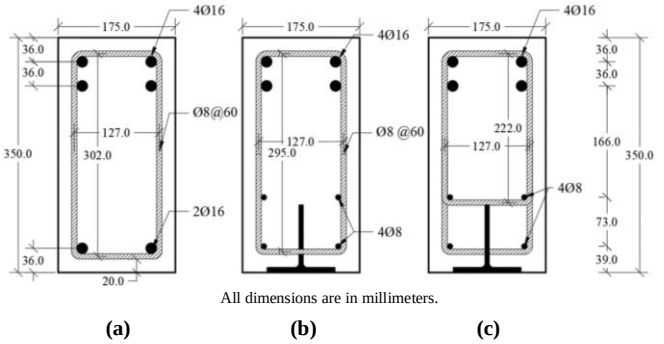

Fig. 3 Cross-section details, **(a)** RC beam, **(b)** CRC beam with 100 % degree of shear connection, **(c)** CRC beam with degree of shear connection less than 100 %.

2.2. Materials

The concrete mix was made with Portland cement, natural sand and crushed gravel of 19 mm maximum size. Superplasticizer was used to obtain good workability of concrete for the required compressive strength. The properties of concrete are given in Table 2. The concrete control specimens were prepared and cured in the same manner as the test beams, and they were tested on the same day of testing the beams.

Steel T-section was used to fabricate the test beams. The section dimensions were 100 mm flange width with 7 mm thickness and 100 mm total depth with 5 mm web thickness.

Tension test coupons were cut from the flange and web of the section. The average properties of steel are shown in Table 2.

The longitudinal reinforcement and stirrups were of 16 mm and 8 mm deformed bars. Tension tests were carried out on specimens cut from the used quantity and the average properties obtained for the two dimeters are shown in Table 2.

Table 2. Properties of used materials.

Material	Properties	Values
Concrete	Elastic modulus, MPa	25570
	Poisson's ratio	0.2
	Compression strength (cylinder), MPa	29.6
16 mm reinforcement bars	Elastic modulus, MPa	201282
	Poisson's ratio	0.3
	Ultimate tensile strength, MPa	636
	Yield strength, MPa	527
8 mm reinforcement bars	Elastic modulus, MPa	202150
	Poisson's ratio	0.3
	Ultimate tensile strength, MPa	490
	Yield strength, MPa	314
Steel T-section	Elastic modulus, MPa	204263
	Poisson's ratio	0.3
	Ultimate tensile strength, MPa	508
	Yield strength, MPa	376

2.3. Test setup, instrumentation and test procedure

The test setup is shown in Figs. 4 and 5. The test rig was built with the aim to subject a concentrated force at mid span of the curved in plan beam. Each beam was provided with concrete block at its two ends. These blocks were well designed in order not to fail during the test, and to provide fixed supports at the beam ends. The blocks were held to the test rig by using four 40 mm bolts and a supporting steel device. Each steel device consisted of two I-section welded side to side and strengthened with steel stiffeners.

The rig was equipped with 1000 kN loading hydraulic piston that provided the load at mid span of the beam. The load was applied through a circular steel plate of 200 mm diameter and 20 mm thickness, connected to a hinge to allow for small rotation. The hydraulic oil pressure in the piston was calibrated by using a load cell. The calibration was made before testing to determine the relation between the hydraulic oil pressure and the load, the equation obtained from the calibration was implemented in the software of the data logger to record the load applied through the piston instead of the pressure.

Electrical resistance strain gauges were used to measure the strains in concrete and steel. Strain gauges with gauge length of 60 mm were used for concrete and gauge length of 5 mm for the steel T-section. Four strain gauges were installed at mid-span, three on concrete across the depth of the section of the beam and one on the soffit of steel T-section, to measure the strain distribution at mid span, another strain gauge was installed on the soffit of the steel T-section at the support to measure the compressive strain in the T-section. One strain gauge rosette was also used on the surface of concrete at approximately one forth span length, where the twisting moment is maximum as determined by the elastic analysis in Appendix 1. Fig. 6 depicts the distribution of strain gauges.

The strain in reinforcement was assumed to be equal to the strain on the concrete surface at the location of reinforcement for both longitudinal bars and stirrups. The beams were tested with the load applied incrementally. After each increment all instrument readings were recorded and cracks were marked. Failure load was defined as the load at which the deformation increased with constant load.

The mid span deflection was measured using a 50 mm dial gauge, also the mid span twisting angle was measured using two 30 mm dial gauges installed 200 mm apart across the depth of the section at mid span as shown in Figs. 4 and 5.

Fig. 4 Testing rig with beam C4.

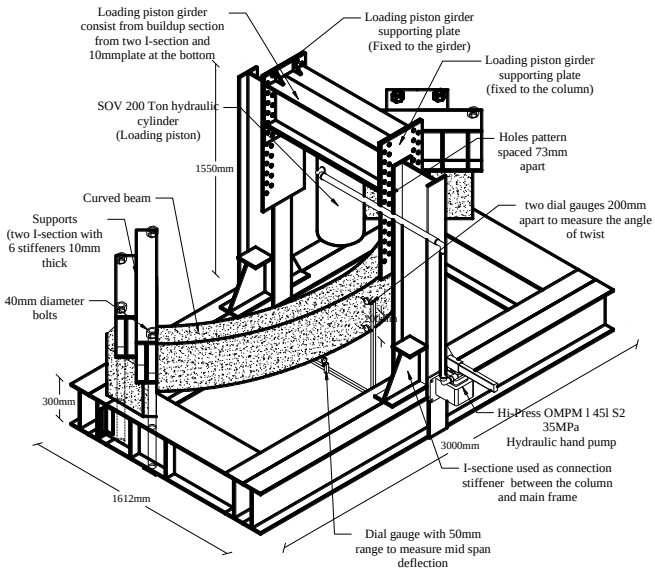

Fig. 5 Details of test rig with the beam specimen.

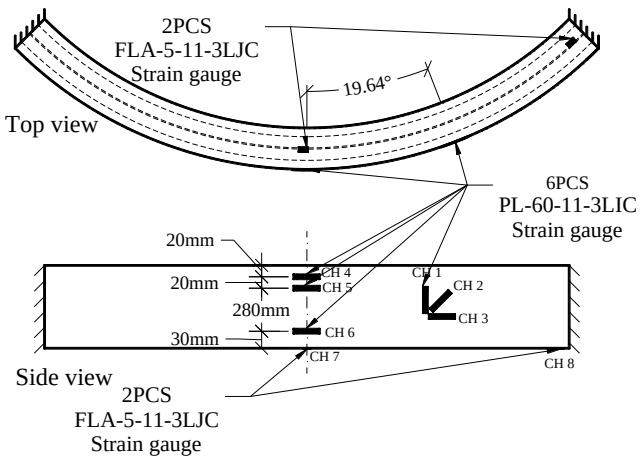

Fig. 6 Distribution of strain gauges.

2.4. Failure modes.

Figure 7 shows specimen C1 failure, and as can be seen the failure is by flexure due to the reinforcement yielding at mid span at load equal to 212 kN. After this load value the mid span deflection increases with a decrease in the load value indicating failure. The failure of the beam started with the yield in the 8 mm stirrups at load equal to 118.9 kN. The 16 mm bars reached their yield stress at load equal to 186.1 kN.

Fig. 7 Specimen C1 failure.

The failure of specimen C2 with 100 % degree of shear connection between the concrete and steel T-section was due to torsion and shear effects as shown in Fig. 8. The two-piece C-shaped stirrups reached their yield stress at load equal to 188.2 kN. Helical cracks formed along the beam and finally led to failure of beam at the supports. The maximum load of the beam was 214 kN which is approximately equal to that of the RC beam C1.

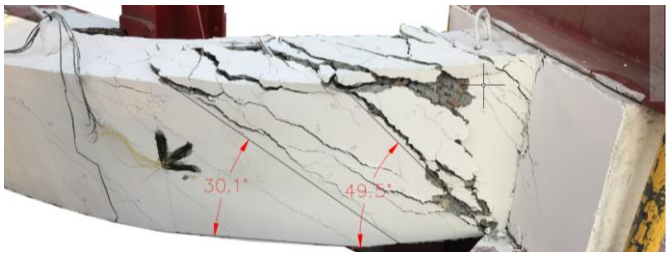

Fig. 8 Specimen C2 failure.

The CRC beam C3 with 67.4 % degree of shear connection exhibited the same failure mode as that of specimen C2 but the failure was at one forth the span where the twisting moment is maximum as shown in Fig. 9. The beam ultimate load capacity was 277.4 kN which is 31 % and 30 % larger than those for beams C1 and C2 respectively.

The strain values showed that the 8 mm stirrups reached yield stress at load equal to 184.9 kN, then the 8 mm longitudinal bars reached the yield point at mid span at load equal to 191.8 kN followed by the yield of the steel T-section at load equal to 205.8 kN.

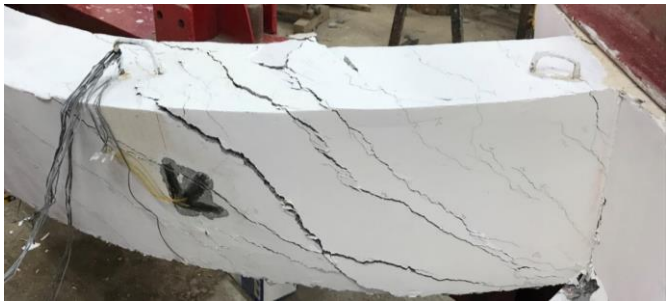

Fig. 9 Specimen C3 failure.

Figure 10 shows the failure mode for CRC beam C4 with 48.8 % degree of shear connection. The failure changed from shear and torsion to flexural failure at the supports followed by torsion failure with severe cracks at the maximum torsion zone as shown in Fig. 10. The beam attained an ultimate load value of 329 kN which is 55 %, 54 %, and 19 % larger than those for beams C1, C2, and C3 respectively.

The strain values showed that the 8 mm longitudinal bars reached their yield stress at mid span at load equal to 219 kN, followed by yielding of the 8 mm stirrups at load equal to 260 kN. At maximum load the compressive strain in the steel T-section at the support reached 99 % of its yield stress.

Fig. 10 Specimen C4 failure.

The last beam in this group is CRC beam C5 with 25.6 % degree of shear connection which failed in shear and torsion with maximum load carrying capacity value of 206 kN. The failure mode for this beam is shown in Fig. 11. The strain values showed that the 8 mm stirrups reached their yield stress at load equal to 99.26 kN and then the steel T-section reached its yield stress in compression at the support at load equal to 184 kN.

The ultimate loads, maximum deflections, maximum twisting angles, and first crack loads for the tested beams are listed in Table 3.

Fig. 11 Specimen C5 failure.

Table 4 shows the failure mode of the beams. Using the equations obtained from the linear analysis in Appendix 1, the maximum bending moments at mid span and support and the twisting moments at support and the maximum are calculated by considering the experimental failure load and the results are given in the table.

Table 4 also contains the results of previous studies conducted by the authors Witwit and Jasim [4] and [5]. Witwit and Jasim, 2021 investigated experimentally and numerically the behaviour of straight beams made of this structural material under sagging and hogging bending. The cross section and materials properties were exactly similar to those used in the current study on curved beams. Only two degrees of shear connection were examined, 100 % and 48.8 %.

Table 3. Ultimate load, maximum deflection, maximum twisting angle, and first crack load for the tested beams.

Beam designation	Degree of shear connection (No. of stirrup connectors)	Ultimate load kN.	Ultimate load ratio	Service load kN.	Max. deflection mm	Max twist angle Degree	First crack load kN.
C1	Reinforced concrete	212.0	1.00	141.3	55.8	8.0	50.5
C2	100 (43)	214.0	1.01	142.7	101.6	9.2	50.0
C3	67.4 (29)	277.4	1.31	184.9	105.8	10.7	47.0
C4	48.8 (21)	329.0	1.55	219.3	101.6	6.8	20.0
C5	25.6 (11)	206.0	0.97	137.3	67.2	6.4	39.0
Service load is 2/3 the maximum load							

The bending strength capacities in sagging and hogging regions were determined. These values are given in 8th and 9th columns of Table 4. Also, Witwit and Jasim, 2021, investigated experimentally and numerically the behaviour of CRC beams under pure torsion. Z-shaped beams with the same cross section and material properties were tested. Only two degrees of shear connection were examined, 100 % and 48.8%. The torsional strength capacity was determined as given in 7th column of table 4.

The results of ultimate loads from Table 3 and bending and torsional moments from Table 4, for curved beams, show that the degree of shear connect have no effect on the behaviour of the beams. Even beam C5, which had 25.6 % degree of shear connection, gave load and moment capacity approximately equal to values obtained from beam C2 with 100 % degree of shear connection. This proves the efficiency of the stirrups in providing the connection between the reinforced concrete component and the steel T-section.

From Table 4 it is clear that the values of twisting moments at supports, -T, for beams C2 and C4 in addition to RC beam C1 are less than the torsional strength capacities obtained from testing Z-shaped beams under pure torsion. This reveals that the presence of flexure dose not increase the torsional strength of CRC in contrast to what have been found for normal composite beams [9].

Also, Table 4 shows that the values +M = 62.9 kN.m and -M = -80.4 kN.m developed in beam C2 are considerably less than the bending strength capacities $+M_{max}$ and $-M_{max}$ achieved from testing straight beams. This is due to that the failure of this beam is due to torsion and shear. However, for beam C4 in which the failure is due to bending at the support, the hogging bending moment, -M, attains a value of -126 kN.m which is larger than the capacity of the straight beam, -108 kN.m.

The beam C3 failed due to torsion and shear at region of maximum torsional moment, +T, at an angle of 19.61 degree from mid-span axis. The calculated value of bending moment at this point nearly zero (-0.07 kN.m).

The maximum torsional moment for this beam is 14.1 kN.m as shown in Table 4. This value is small as compared to 21.25 kN.m and 24.25 kN.m for Z-shaped beams with 100 % and 48.8 % degrees of shear connection, keeping in mind that the degree of shear connection of beam C3 is 67.4 %.

The values of bending moments and corresponding torsional moments in Table 4 illustrate that bending-torsion interaction equation exists, but the presence of any action reduces the capacity to resist the other.

Table 4. Failure mode and the corresponding flexural and torsional moments.

Beam	Failure mode	Linear analysis results for curved beams				Straight and Z-shaped beam results		
		kN.m				kN.m		
		+M	-M	+T	-T	T_{max}	$+M_{max}$	$-M_{max}$
C1	Flexure at mid-span	60.6	-81	10.2	8.6	19.11	81.03	-
C2	Torsion +Shear	62.9	-80.4	10.9	7.3	21.25	147.3	-108
C3	Torsion +Shear	81.6	-104.1	14.1	9.4	-	-	-
C4	Negative moment +Torsion	96.7	-123.5	16.8	11.1	24.25	143	-108
C5	Torsion +Shear	60.6	-77.3	10.5	7.0	-	-	-
+M: maximum positive moment, -M: maximum negative moment, +T: maximum torque at quarter span,-T: torque at supports, $+M_{max}$, $-M_{max}$: maximum flexural capacity of the beam in sagging and hogging test from the experimental test of [4], T_{max}: Maximum section torque capacity from experimental test of [5].								

2.5. Load deflection behaviour

Figure 12 shows the load mid-span deflection relationships for the beams. The tangent stiffness of the beam for uncracked section and the secant stiffness at service load are calculated and the results are listed in Table 5. The results depict that the CRC beam C4 has the maximum tangent and secant stiffness when compared to the other CRC beams, although the degree of shear connection for this beam is 48.8%. The behaviour of beam C5, with 25.6 % degree of shear connection, is approximately the same of that of beam C2, with 100 % degree of shear connection, as shown in Fig. 12. This boosts the conclusion that the degree of shear connection has no effect on the behaviour of the CRC beams.

Table 5 shows that decreasing the degree of shear connection from 100 % to 48.8 % increased the stiffness of the beam by 1.15 and 1.25 times for tangent and secant stiffness values respectively. This may be due to the increase in torsional strength of the beam C4 by using more closed stirrups in the beam.

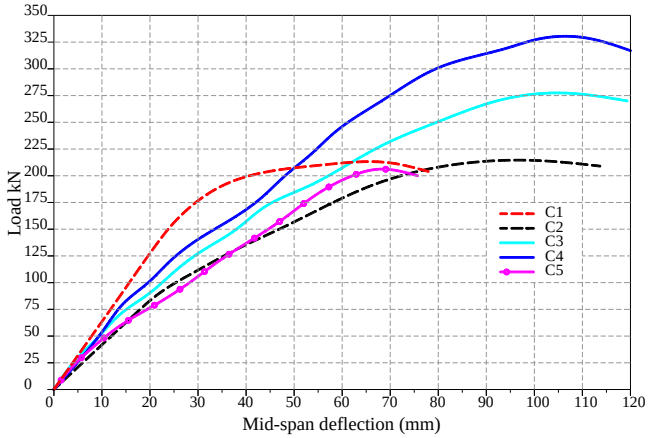

Fig. 12 Load deflection relationships for the tested beams.

Table 5. Tangent and secant stiffness values for the tested beams.

Beam designation	Degree of shear connection (No. of stirrups)	Tangent stiffness K_T	Secant stiffness K_S	$\frac{K_S}{K_T}$ %
C1	Reinforced concrete	6.42	6.33	99 %
C2	100 (43)	4.18	3.23	77 %
C3	67.4 (29)	4.53	3.62	80 %
C4	48.8 (21)	4.80	4.04	84 %
C5	25.6 (11)	3.96	3.41	86 %

Figure 13 shows the experimental load mid-span twisting angle relationships for the five tested beams. The figure shows that the slope of these relationships are the same up to the cracking of concrete. After concrete cracking the slope varies for the different beams. The largest slop is for beam C4 and then beam C3 and then beam C5. Beam C2 with 100 % degree of shear connection reveals a behaviour different from those for other CRC beams.

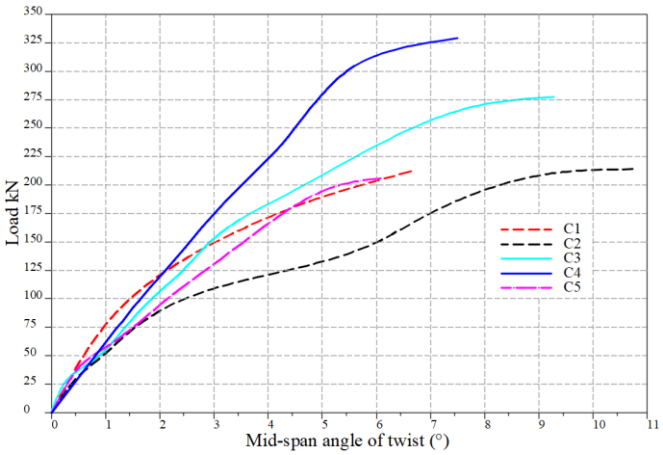

Fig. 13 Load mid-span twisting angle relationships for the tested beams.

3. Finite element analysis

The RC and CRC curved in plan beams were modelled using finite element analysis software ABAQUS [12]. A 20-node brick element C3D20R is used from the element library of ABAQUS to model the concrete, steel T-section, 8 mm stirrups, 8 mm bars, and 16 mm bar. The beam boundary conditions are shown in Fig. 14.

A mesh convergency study has been conducted by changing the element size until no further influence on the results of the load-deflection relation is obtained. The relation between the number of elements and maximum deflection for beam C2 is shown in Fig. 15. The final size of elements selected for the concrete is (9.4 × 10 × 10 mm) as shown in Fig. 16.

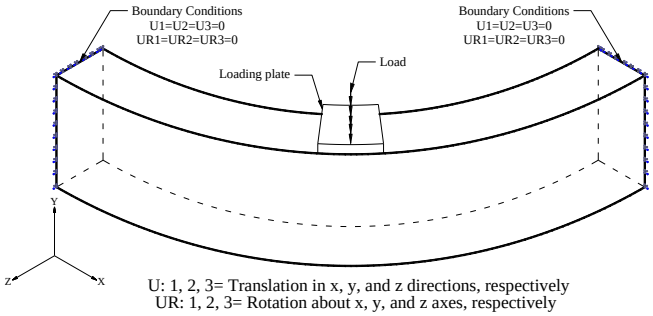

Fig. 14 Beam boundary conditions.

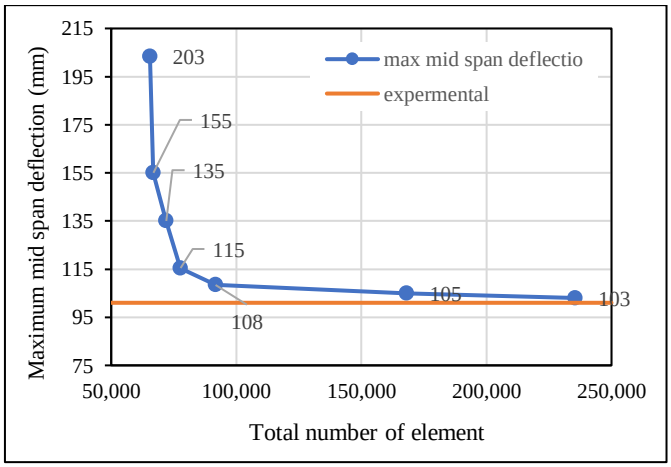

Fig. 15 Midspan deflection vs. element number for specimen C2.

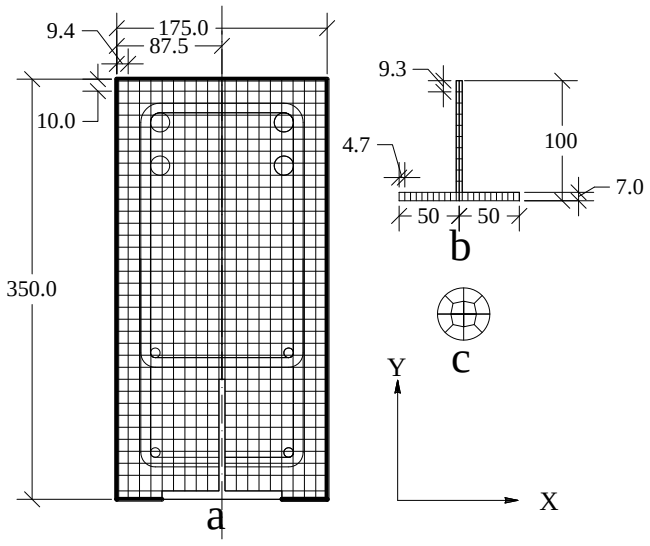

Fig. 16 Mesh size for beams (All dimensions are in millimeters).

The element size for the steel T-section is shown in Fig. 16 (b). The length in radial direction, is 50 mm. The discretization of the 8 mm and 16 mm bars is shown in Fig. 16 (c). The element lengths are 20 mm and 40 mm for the two bar sizes 8 mm and 16 mm, respectively. The aspect ratio for all elements is kept to be about 10. The total number of elements for this model was 235528.

4. Material modelling

4.1. Concrete

Elastic-plastic behaviour that includes softening has been used according to Carreira and Chu [13] to model concrete in compression. The model used was concrete damage plasticity. The parameters of the concrete model are listed in Table 6. The stress-strain relationship for concrete in tension was assumed linear up to the point of concrete cracking at a tensile stress of 10 % of concrete compressive strength. After the concrete cracking, the tensile stress decreases linearly to zero at a strain equal to 10 times the strain at cracking. The ratio of the second stress invariant on the tensile meridian, to that on the compressive meridian K was taken 0.667. The ratio of ultimate biaxial compressive stress, f_{b0} , to uniaxial compressive stress f_{c0} was used as 1.16.

Table 6. Material parameters of Concrete damage plasticity model.

Parameters	Values
Concrete compressive strength $f'c$	29.6 (MPa)
Concrete tensile strength	1.56 (MPa)
Modulus of elasticity (E)	25570 (MPa)
Poisson ratio (v)	0.19
Dilation angle (β)	36°
$f = f_{b0}/f_{c0}$	1.16
K	0.667

4.2. Steel

The Elastic-plastic model is used to model the behaviour of all types of the steel. The values of yield stress and ultimate strength of the steel T-section and reinforcement bars are as listed in Table 2.

4.3. Interaction between beam components

Different surface-to-surface contacts were used to ensure that the model behaves in a way that captures the actual behaviour of the CRC beam. The steel reinforcements contact to concrete were modelled using embedded region model.

The loading plate contact to the surface of the concrete has two directions the first one is the normal contact which is modelled as hard contact that allows separation, and the second one is the tangential behaviour which was modelled as rough surface thus not allowing for any slip between the loading plate and the concrete surface.

The normal contact between concrete and steel T-section was modelled as hard contact that allows separation.

In the new composite reinforced concrete, the shear connection is provided throughout the length of the beam by relying on the stirrups which pass through drilled holes in the web of the steel T-section. The shear connection transmits the longitudinal shear force between the steel T-section and the concrete component of the beam, in addition to prevent the separation between the two components. In the finite element model the shear connection was modelled by using a linear spring element of zero length with specified stiffness.

The positions of the spring elements coincided with the positions of the stirrups. Three springs in the three directions x, y, and z were used in each position. The stirrups were cut and connected to the web of the steel T-section by the spring elements on both sides of the web. The stiffness used in the model was based on the values mentioned in [1], [2], [14], [15], and [16]. The chosen value for spring stiffness was 428 kN/mm.

5. Finite element model validation

In order to validate the suggested finite element model, comparison with the experimental results of tested beams was made. The finite element model and experimental results are compared in Figs. 12 to 16 in terms of load-mid span deflection relationships. The figures depict excellent agreement in the response over the entire loading profile until failure.

Table 6 summarizes the comparison between the model and test results in terms of the maximum load carrying capacity of the beams. The ratios of results, experimental to model, are approximately one indicating good predictions of the strength and the deflection.

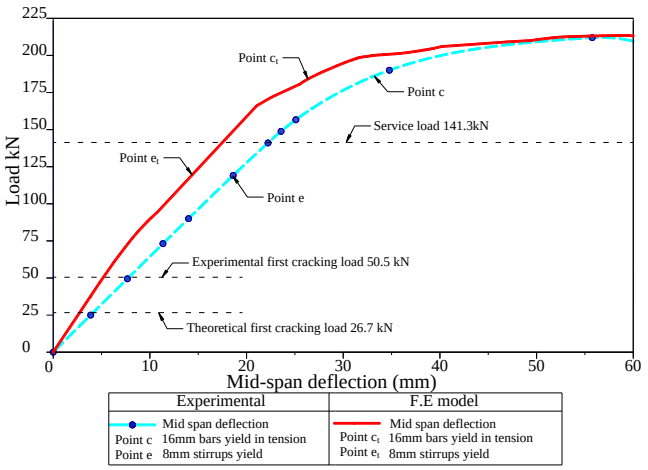

Fig. 17 Variation of mid span deflection with load for beam C1.

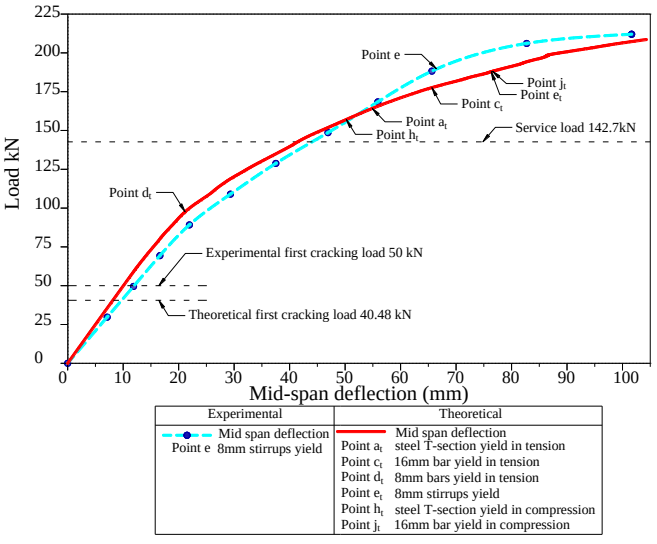

Fig. 18 Variation of mid span deflection with load for beam C2.

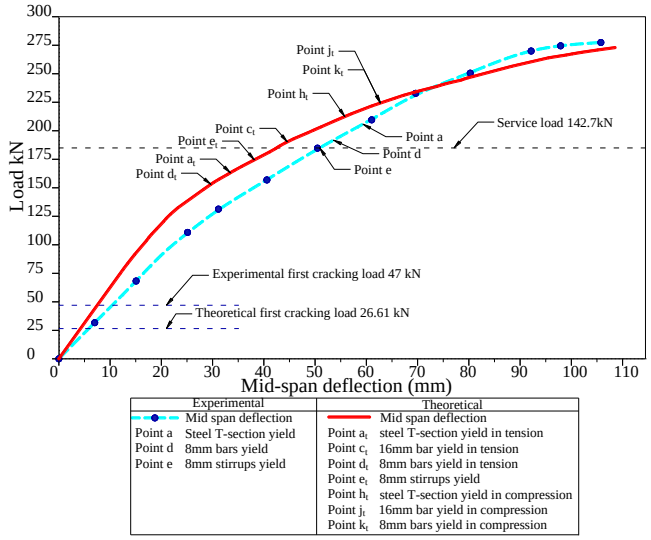

Fig. 19 Variation of mid span deflection with load for beam C3.

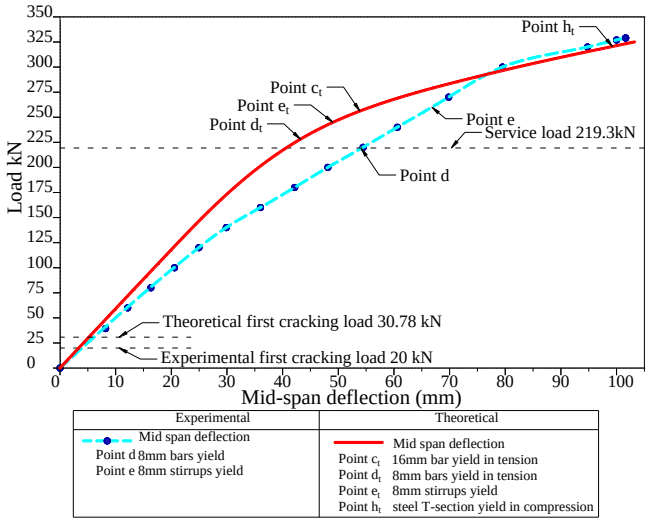

Fig. 20 Variation of mid span deflection with load for beam C4.

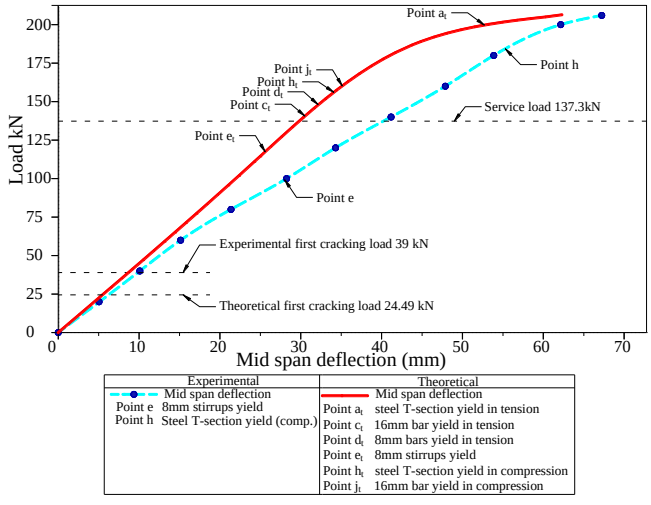

Fig. 21 Variation of mid span deflection with load for beam C5.

Table 7. Experimental and F.E model load and deflection results for the tested beams.

Beam designation	Experimental results		F.E model results		$\frac{P_{ex}}{P_{FE}}$	$\frac{\Delta_{Ex}}{\Delta_{FE}}$
	Maximum load P_{ex} kN.	Deflection at maximum load Δ_{ex} mm	Maximum load P_{FE} kN.	Deflection at maximum load Δ_{FE} mm		
C1	212.0	55.8	213.55	58.80	0.99	0.95
C2	214.0	101.6	208.56	104.30	1.03	0.97
C3	277.4	105.8	272.92	108.53	1.02	0.97
C4	329.0	101.6	325.01	103.20	1.01	0.98
C5	206.0	67.2	206.40	62.28	1.00	1.08

5. Conclusions

A new competitive structural material, in which a steel T-section is connected to and acts as a reinforcement with concrete component, is proposed. The connection between the steel T-section and the concrete component is provided by the stirrups that are required to resist shear and torsion acted on the beam. The stirrups are made of two C-shaped pieces and pass-through holes drilled in the web of the steel T-section. The experimental results show that the stirrups are very effective as shear connectors for this type pf composite reinforced concrete CRC beams. The degree of shear connection is found to have no effects on the behaviour of the tested curved in plan beams.

1. As compared to ordinary reinforced concrete beam, the CRC beams show an increase in ultimate load capacity which my reach 55 %.
2. A three-dimensional finite element model using the software ABAQUS is proposed to simulate the behaviour of the curved in plan beams under mid-span concentrated load.
3. A comparison of the experimental and numerical results relating to ultimate loads, maximum deflections and load mid-span relationships shows reasonable agreement.

References

[1] R. Taylor, and P. Cunningham, “Tests on the transverse bar shear connector for composite reinforced concrete”, Proceedings of the Institution of Civil Engineers, part 2, Vol. 63, Issue 4, pp. 913-920, 1977. https://doi.org/10.1680/iicep.1977.3086

[2] R. Taylor, D. S. E. Clark, and J. J. Nelson, “Test on a new type of shear connectors for composite reinforced concrete”, Proceedings of the Institution of Civil Engineers, Part 2, Vol. 57, pp. 177, 1974. https://doi.org/10.1680/iicep.1974.4107

[3] D. A. U. Witwit, “Experimental and theoretical study on composite reinforced concrete beams curved in plan”, Ph. D. Thesis, Civil Engineering Department, College of Engineering, University of Basrah, Iraq, 2021.

[4] D. A. U. Witwit and N. A. Jasim, “Assessment of the flexural capacity of composite reinforced concrete beams using experimental tests and finite element analysis”, Journal of Physics: Conference Series, Vol. 1895, pp. 1-15, 2021. https://doi.org/10.1088/1742-6596/1895/1/012066

[5] D. A. U. Witwit and N. A. Jasim, “Torsional Capacity of Composite Reinforced Concrete Beams with Stirrup Connectors”, Anbar Journal of Engineering Sciences, Vol. 12, Issue 2, pp. 177-192, 2021. https://doi.org/10.37649/aengs.2021.171186

[6] V. Thevendran, N. E. Shanmugam, S. Chen, J. Y. R. Liew, "Experimental study on steel-concrete composite beams curved in plan", Engineering Structures, Vol. 22, Issue 8, pp. 877-889, 2000. https://doi.org/10.1016/S0141-0296(99)00046-2
[7] E. L. Tan, and B. Uy, "Experimental study on straight composite beams subjected to combined flexure and torsion", Journal of Constructional Steel Research, Vol. 65, Issue 4, pp.784-793, 2009. https://doi.org/10.1016/j.jcsr.2008.10.006
[8] E. L. Tan, and B. Uy, "Nonlinear analysis of composite beams subjected to combined flexure and torsion", Journal of Constructional Steel Research, Vol. 67, Issue 5, pp. 790-799, 2011. https://doi.org/10.1016/j.jcsr.2010.12.015
[9] E. L. Tan, and B. Uy, "Experimental study on curved composite beams subjected to combined flexure and torsion", Journal of Constructional steel research, Vol. 65, Issue 8-9, pp. 1855-1863, 2009. https://doi.org/10.1016/j.jcsr.2009.04.015
[10] V. Thevendran, S. Chen, N. E. Shanmugam, and J. Y. R. Liew, "Nonlinear analysis of steel-concrete composite beams curved in plan", Finite Elements in Analysis and Design, Vol. 32, Issue 3, pp. 125-139, 1999. https://doi.org/10.1016/S0168-874X(99)00010-4
[11] B. Ghosh and S. Mallick, "Strength of steel-concrete composite beams under combined flexure and torsion", Indian Concrete Journal, Vol. 53, No. 2, pp. 48-53, 1979.
[12] D. S. Simulia, "Abaqus 6.14", Abaqus 6.14 Analysis User's Guide, 2014.
[13] D. J. Carreira and K. H. Chu, "Stress-Strain Relationship for Plain Concrete in Compression", ACI Journal Proceedings, Vol. 82, Issue 6, pp. 797-804, 1985. https://doi.org/10.14359/10390
[14] J. Hegger, P. Döinghaus, "High performance steel and high performance concrete in composite structures", Composite Construction in Steel and Concrete IV, pp. 891-902, 2000. https://doi.org/10.1061/40616(281)77
[15] C.-S. Shim, P.-G. Lee, and T.-Y. Yoon, "Static behavior of large stud shear connectors", Engineering Structures, Vol. 26, Issue 12, pp. 1853-1860, 2004. https://doi.org/10.1016/j.engstruct.2004.07.011
[16] A. Prakash, N. Anandavalli, C. K. Madheswaran, N. Lakshmanan, "Modified push-out tests for determining shear strength and stiffness of HSS stud connector-experimental study", International Journal of Composite Materials, Vol. 2, Issue 3, pp. 22-31, 2012. https://doi.org/10.5923/j.cmaterials.20120203.02
[17] ACI Standard, Reported by ACI Committee 318, "Building code requirements for structural concrete and commentary (ACI 318-19)", Farmington Hills, MI, USA, 2019. https://doi.org/10.14359/51716937

Appendix 1: Elastic analysis

Figure 22 shows a free body diagram for a segment of the curved in plan beam subtended an angle π/2 and subjected to a concentrated force applied to it at mid-span. The moment and torsion at any angle θ, measured from the mid-span, can be calculated as follows:

$$M_\theta = M_A \cos\theta - \frac{P}{2} R \sin\theta \quad (1)$$

$$T_\theta = M_A \sin\theta - \frac{P}{2}(R - R\cos\theta) \quad (2)$$

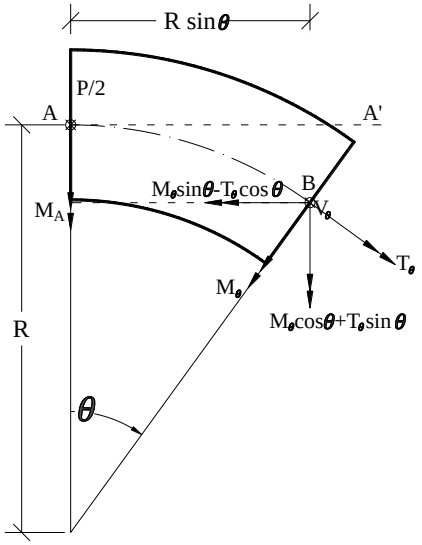

Fig. 22 Free body diagram for horizontally curved beam.

To determine M_θ and T_θ the moment M_A at mid-span must be calculated. The strain energy U of the beam is given by:

$$U = 2\int_0^{\pi/4} \frac{M_\theta^2}{2EI}\, ds + 2\int_0^{\pi/4} \frac{T_\theta^2}{2GJ}\, ds \quad (3)$$

Where: EI is the flexural rigidity and GJ is the torsional rigidity. Due to symmetry, the rotation at mid span is zero.

$$\therefore \frac{\partial U}{\partial M_A} = 0$$

$$\therefore 0 = 2\int_0^{\pi/4} \frac{2M_\theta}{2EI} \times \frac{\partial M_\theta}{\partial M_A} \times ds + 2\int_0^{\pi/4} \frac{2T_\theta \dfrac{\partial T_\theta}{\partial M_A}}{2GJ}\, ds$$

$$\therefore 0 = 2\left[\int_0^{\pi/4} \frac{\left\{M_A\cos\theta - \frac{P}{2} R\sin\theta\right\}\cos\theta\ R}{EI}\, d\theta + \int_0^{\pi/4} \frac{\left\{M_A\sin\theta - \frac{P}{2}(R - R\cos\theta)\right\}\sin\theta\ R}{GJ} d\theta\right]$$

$$\therefore \frac{R}{EI}\int_0^{\pi/4}\left[M_A\left(\frac{1+\cos 2\theta}{2}\right) - \frac{PR}{2}\sin\theta\cos\theta\right] d\theta + \frac{R\propto}{EI}\int_0^{\pi/4}\left[M_A\left(\frac{1-\cos 2\theta}{2}\right) - \frac{RP}{2}\sin\theta + \frac{PR}{2}\sin\theta\cos\theta\right] d\theta = 0 \qquad \left[\text{where } \propto = \frac{EI}{GJ}\right]$$

$$\therefore \frac{R}{EI}\left[\frac{M_A}{2}\left(\theta + \frac{1}{2}\sin 2\theta\right) + \frac{PR}{2}\frac{\cos 2\theta}{4}\right]_0^{\pi/4} + \frac{R\propto}{EI}\left[\frac{M_A}{2}\left(\theta - \frac{1}{2}\sin 2\theta\right) + \frac{PR}{2}\cos\theta - \frac{RP}{2}\frac{\cos 2\theta}{4}\right]_0^{\pi/4} = 0$$

$$\therefore \frac{M_A}{2}\left(\frac{\pi}{4}+\frac{1}{2}\right)+\alpha\left[\frac{M_A}{2}\left(\frac{\pi}{4}-\frac{1}{2}\right)+\frac{PR}{2}\frac{1}{\sqrt{2}}\right] - \left[\frac{PR}{2}\frac{1}{4}+\alpha\left\{\frac{PR}{2}-\frac{PR}{2}\frac{1}{4}\right\}\right]=0$$

$$\therefore \frac{M_A}{2}\left(\frac{\pi+2}{4}\right)+\alpha\frac{M_A}{2}\left(\frac{\pi-2}{4}\right)+\alpha\frac{PR}{2\sqrt{2}}-\frac{PR}{8} - \alpha\frac{PR}{2}+\alpha\frac{PR}{8}=0$$

$$\therefore M_A(\pi+2)+\alpha M_A(\pi-2)+2\sqrt{2}\,\alpha PR-PR - 4\alpha PR+\alpha PR=0$$

$$\therefore M_A=\frac{PR(0.172\,\alpha+1)}{(5.142+1.142\,\alpha)} \quad (4)$$

The modulus of elasticity of concrete is given by (ACI 318-19):

$$E_c=4700\sqrt{f'c}=4700\sqrt{29.6}=25570\text{ MPa}$$

From elasticity theory (for concrete rectangular section), torsional rigidity is:

$$GJ=G\,\beta\,a\,b^3 \quad (5)$$

where a and b are cross section dimensions and β is a coefficient.

$$G=\frac{E_C}{2(1+v_c)}=\frac{25570}{2(1+0.15)}=11.12\times10^3$$

where Poisson's ratio $v_c=0.15$

From Fig. 23 (with a/b = 350/175 = 2) the value of β can be found as:

$$\beta=0.229\,,\quad \therefore J=0.229\left[350\times175^3\right]=429.55\times10^6\text{ mm}^4$$

To calculate I_x for the beam, the area of the steel needs to be multiplied by transformation factor n which is the ratio of modulus of elasticity of steel divided by the modulus of elasticity of concrete as follow:

$$E_s=200000\text{ MPa}$$

$$n=\frac{E_s}{E_c}=\frac{200000}{25570}=7.82$$

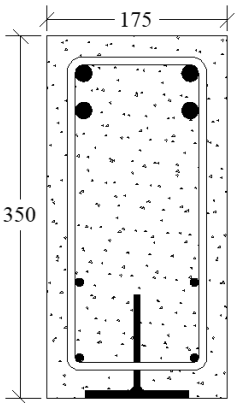

a/b	β
1	0.141
1.5	0.196
2	0.229
2.5	0.249
3	0.263
4	0.281
5	0.291
10	0.312

Fig. 23 Cross section dimensions and β values.

Assuming the cross section as singly reinforced with the steel T-section as the reinforcement, the neutral axis of the cracked section is given by:

$$\frac{bx^2}{2}-n.\,A_{ST}\,(d-x)=0 \quad (6)$$

where A_{ST} = area of steel T-section = 1165 mm^2, d = effective depth of section = 350 - 23.46 = 326.5 mm and b = 175 mm.

Substituting into *Eq.* (6) gives: x = 139.5 mm

The moment of inertia I_x for the cracked section is given by:

$$I_x=\frac{bx^3}{3}+I_{xT}\,n+n\,A_{ST}\,(d-x)^2 \quad (7)$$

where I_{xT} = moment of inertia for steel T-section about its own x-centroidal axis = 1036505 mm^4.

Substituting into *Eq.* (7) gives: $I_x=4.8504\times10^8$ mm^4

$$\therefore \alpha=\frac{EI}{GJ}=\frac{25570\times4.8504\times10^8}{11.12\times10^3\times429.55\times10^6}=2.597$$

Substituting the value of (α) into *Eq.* (4) gives the value for M_A as:

$$M_A=\frac{PR(0.172\times\alpha+1)}{(5.142+1.142\,\alpha)}= \frac{P\times1.65(0.172\times2.597+1)}{(5.142+1.142\times2.597)}=0.294P\text{ (in kN.m when } P\text{ in kN)}$$

Substituting the value of M_A in equations 1 and 2, the bending moment M_θ, and twisting moment T_θ at any point can be calculated.

As an example, for load of 250 kN, the internal forces and moments at various sections at mid-span, $\theta=0$.

$$\therefore M_\theta=M_A=0.294\,P=73.5\text{ kN.m}$$

$$T_\theta=0,\ V_\theta=\frac{P}{2}=125\text{ kN}\quad\text{at support, }\theta=\pi/4$$

$$M_\theta=-\,93.87\text{ kN.m}\,,\quad T_\theta=-\,8.44$$

The maximum twisting moment occurs at $\theta=19.614°$.

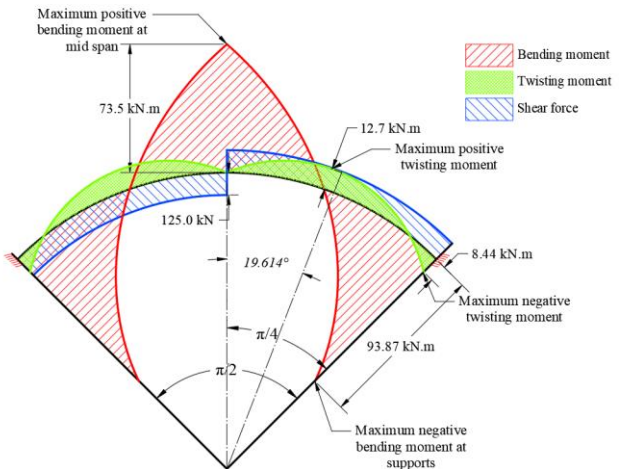

Fig. 24 Shear force, twisting moment, and bending moment diagrams for a horizontally curved beam under 250 kN concentrated force at mid-span.